

## Features of incommensurate phases in $K_2SeO_4$ , $K_2ZnCl_4$ , and $Rb_2ZnCl_4$

Y. Koyama

*Kagami Memorial Laboratory for Materials Science and Technology, Waseda University, Nishiwaseda, Shinjuku-ku, Tokyo 169, Japan; Advanced Research Center for Science and Engineering, Waseda University, Ohkubo, Shinjuku-ku, Tokyo 169, Japan; and Department of Materials Science and Engineering, Waseda University, Ohkubo, Shinjuku-ku, Tokyo 169, Japan*

T. Nagata and K. Koike

*Department of Materials Science and Engineering, Waseda University, Ohkubo, Shinjuku-ku, Tokyo 169, Japan*

(Received 29 December 1994)

Among the  $A_2BX_4$  family, features of incommensurate phases in  $K_2SeO_4$ ,  $K_2ZnCl_4$ , and  $Rb_2ZnCl_4$  have been examined using a Ginzburg-Landau theory with complex amplitudes of the first- and higher-order lattice distortions as an order parameter. Characteristic features of the present theory are that the theory is based on an extended-zone scheme and only higher-order distortions with wave vectors close to a vector of the first-order one are taken into account. Free energies of incommensurate and commensurate phases then have the third-order umklapp and lock-in terms, respectively, from an invariance of the translational symmetry. Note that neither a polarization wave in the incommensurate phase nor a macroscopic polarization in the commensurate one is considered. In spite of this neglect, the present theory can sufficiently reproduce incommensurate features such as a change in an incommensurability and a phase modulation. That is, the incommensurate features in these materials are understood to originate mainly from the phase modulation of the first-order distortion by means of the higher-order ones.

### I. INTRODUCTION

A lot of normal-incommensurate-commensurate transitions have been so far reported in the dielectric  $A_2BX_4$  family. Among the  $A_2BX_4$  family, potassium selenate  $K_2SeO_4$  is a prototypical material and exhibits a normal-to-incommensurate transition at  $T_I$  of 130 K and an incommensurate-to-commensurate one at  $T_c$  of 91 K.<sup>1,2</sup> Features of the incommensurate structure are that a direction of a modulation is parallel to the  $c$  axis and its period is close to a commensurate value of  $3c_0$  where lattice parameters of the normal orthorhombic phase (space group;  $Pcmn$ ) were determined to be  $a_0=10.466$  Å,  $b_0=6.003$  Å, and  $c_0=7.661$  Å.<sup>3</sup> Note that ferroelectric properties are obtained only in the commensurate phase with the period of  $3c_0$ . The same type of successive transitions have been also found in  $K_2ZnCl_4$  and  $Rb_2ZnCl_4$ .<sup>4-10</sup> The present theory described here focuses on the incommensurate phases in these materials as well as  $K_2SeO_4$ .

Features of the incommensurate phases in  $K_2SeO_4$ ,  $K_2ZnCl_4$ , and  $Rb_2ZnCl_4$  have been investigated experimentally and basically resemble one another. As for  $K_2SeO_4$ , as an example, a modulation mode of the incommensurate structure has been analyzed to be mainly due to a rotation of the  $SeO_4$  tetrahedron about the  $a$  and  $c$  axes.<sup>1</sup> A wave vector characterizing the incommensurate structure is given as  $\mathbf{k}_0 = \frac{1}{3}(1 + \Delta)\mathbf{G}_{001}$  where  $\Delta$  is an incommensurability and  $\mathbf{G}_{001}$  is a reciprocal-lattice vector along the  $c$  axis. A change in  $\Delta$  with respect to temperature was in details examined by means of neutron diffraction.<sup>1</sup> According to the diffraction experiment,  $\Delta$  has a value of  $\bar{\Delta}=0.09$  at  $T_I$ . When the temperature is

lowered,  $\Delta$  decreases gradually in a higher-temperature region of the incommensurate phase and rapidly in a lower-temperature one.

The neutron diffraction in  $K_2SeO_4$  showed that the second- and third-order peaks exist in reciprocal space of the incommensurate phase, in addition to the first-order superlattice peak due to the first-order lattice distortion. According to the discommensuration theory proposed by McMillan,<sup>11</sup> higher-order lattice distortions produced from these harmonics via the umklapp process mainly modulate a phase of the first-order distortion in order to make a free energy of the incommensurate phase lower. An effective phase modulation is made by higher-order distortions in the vicinity of the first-order one in reciprocal space and results in a phase-slip region, which is called the discommensuration. Among the  $A_2BX_4$  family, the discommensuration has been actually observed in  $K_2ZnCl_4$  and  $Rb_2ZnCl_4$  by transmission electron microscopy.<sup>5,7</sup> However, Iizumi, Axe, and Shirane adopted the third-order distortion far from the first-order one, not the second-order one near it, in a construction of a free energy to explain the transitions in  $K_2SeO_4$ .<sup>1</sup> This is because the third-order distortion produced from the third-order harmonic can play a role of the polarization wave  $Pw$  as a secondary order parameter although there is no macroscopic polarization in the incommensurate phase. In their free energy, then there exists the fourth-order umklapp term of  $Q^3Pw$  where  $Q$  is an amplitude of the first-order lattice distortion as a primary order parameter. An important thing is that their theory can reproduce the change in  $\Delta$  only in a special assumption. As a natural consequence, a serious problem is that the modulation by the third-order distortion never results in a phase modulation. That is, the theory cannot predict the discom-

measurement. In the present work, on the basis of this problem, we adopt the second-order distortion related to the second-order peak appearing near the first-order peak in order to explain the incommensurate features, particularly the details of the phase modulation. It should be remarked that Iizumi, Axe, and Shirane neglected the third-order umklapp term related to the second-order distortion in their theory on the basis of a speculation that this term will not lead to lock-in.<sup>1</sup>

As mentioned above, the commensurate phase has been reported to exhibit the ferroelectric properties.<sup>2,9,12-15</sup> In the case of  $\text{K}_2\text{SeO}_4$ , a spontaneous polarization  $P_s$  appears along the  $b$  axis owing to a displacement of the K atom basically. According to Aiki *et al.*,<sup>2</sup> when the temperature is lowered from the incommensurate phase,  $P_s$  jumps from 0 to a finite value at  $T_c$  and subsequently increases in a form of  $P_s^2 \propto (T_0^p - T)$  with  $T_0^p$  of 102 K in the commensurate phase. In addition, a double hysteresis loop was also observed above  $T_c$ .

In the present paper, a Ginzburg-Landau theory explaining features in the incommensurate phases of  $\text{K}_2\text{SeO}_4$ ,  $\text{K}_2\text{ZnCl}_4$ , and  $\text{Rb}_2\text{ZnCl}_4$  is described. We first show an order parameter for the successive transitions in these materials and then a Ginzburg-Landau free energy including only the contribution of the higher-order lattice distortions near the first-order one in reciprocal space. Both the polarization wave in the incommensurate phase and the spontaneous polarization in the commensurate one are not, on the other hand, taken into account from a purpose of an understanding of a role of the higher-order lattice distortions. Incommensurate features calculated using the present free energy are presented and compared with experimental data in  $\text{K}_2\text{SeO}_4$ ,  $\text{K}_2\text{ZnCl}_4$ , and  $\text{Rb}_2\text{ZnCl}_4$ . On the basis of the comparison between the calculated and experimental results, we finally discuss features of both the incommensurate phases and the incommensurate-to-commensurate transitions in these materials.

## II. ORDER PARAMETER IN THE SUCCESSIVE TRANSITIONS

$\text{K}_2\text{SeO}_4$  is a typical material showing a soft-phonon-mode behavior in the normal orthorhombic phase. It is understood from the neutron diffraction that a related phonon mode is a  $\Sigma_2$  optical mode with a wave vector of  $\mathbf{k} \sim \frac{1}{3}[001]$ .<sup>1</sup> It should be noticed that the  $\Sigma_2$  branch is an extension of the  $\Sigma_3$  acoustic branch in an extended zone. Actually the first-order superlattice peak in the reciprocal space of the incommensurate phase is located in the vicinity of  $\mathbf{G}_{002}/3$ , not around  $\mathbf{G}_{001}/3$ , where  $\mathbf{G}_{002}$  is the 002 reciprocal-lattice vector of the normal orthorhombic structure along the  $c$  axis. Therefore, a wave vector of the incommensurate structure should be given as  $\mathbf{k}_0 = \frac{1}{3}(1 - \delta)\mathbf{G}_{002}$  in the extended-zone scheme where  $\delta$  is given as  $\delta = \frac{1}{2}\Delta$ . It is worth noticing that the same situation is realized in  $\text{K}_2\text{ZnCl}_4$  and  $\text{Rb}_2\text{ZnCl}_4$ , and a sign of  $\delta$  is positive for  $\text{K}_2\text{SeO}_4$  and  $\text{K}_2\text{ZnCl}_4$  and negative for  $\text{Rb}_2\text{ZnCl}_4$ . A real order parameter for the first-order lattice distortion is then given as a real part of a complex order parameter  $\Psi_0(\mathbf{r})$ ,  $\eta_0(\mathbf{r}) = \text{Re}[\Psi_0(\mathbf{r})]$ , where

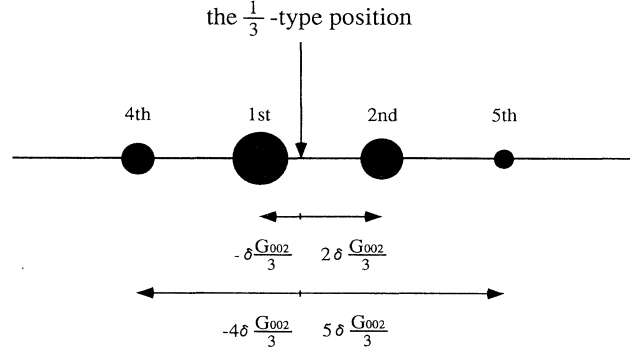


FIG. 1. Schematic representation showing locations of the first- and higher-order spots close to the  $\frac{1}{3}$ -type position,  $\mathbf{G}_{002}/3$ , in electron-diffraction patterns.

$\Psi_0(\mathbf{r}) = \psi_0 \exp(i\mathbf{k}_0\mathbf{r})$  and  $\psi_0$  is a complex amplitude of the complex order parameter.

As mentioned earlier, there exist the second- and third-order peaks in the reciprocal space of the incommensurate phase of  $\text{K}_2\text{SeO}_4$ . The higher-order distortions with wave vectors close to a vector of the first-order distortion can effectively modulate the phase of the first-order one. In electron-diffraction patterns of the incommensurate phases in  $\text{K}_2\text{SeO}_4$ ,  $\text{K}_2\text{ZnCl}_4$ , and  $\text{Rb}_2\text{ZnCl}_4$ , higher-order spots due to the higher-order distortions should appear near the  $\frac{1}{3}$ -type positions,  $\mathbf{G}_{002}/3$ . Figure 1 schematically represents the higher-order spots near the  $\frac{1}{3}$ -type position in the reciprocal space. As is shown in Fig. 1, for instance, the fourth- and fifth-order spots are expected to appear in the vicinity of the  $\frac{1}{3}$ -type position in addition to the second-order spot. Then, the higher-order distortions related to these spots are taken into account in the present theory. Note that the third-order distortion is not considered unlike the theory proposed by Iizumi, Axe, and Shirane.<sup>1</sup> As for locations of the higher-order spots in the reciprocal space, as a vector from the  $\frac{1}{3}$ -type position to the first-order spot is given as  $-\delta\mathbf{G}_{002}/3$ , the second-, fourth-, and fifth-order spots appear at  $+2\delta\mathbf{G}_{002}/3$ ,  $-4\delta\mathbf{G}_{002}/3$ , and  $+5\delta\mathbf{G}_{002}/3$  from the  $\frac{1}{3}$ -type position, respectively. Wave vectors are therefore written as  $\mathbf{k}_j = \frac{1}{3}[1 - (3j+1)\delta]\mathbf{G}_{002} = q_j\mathbf{G}_{002}$  where  $j=0, -1, 1$ , and  $-2$ , correspond to the first-, second-, fourth-, and fifth-order lattice distortions, respectively. A complex order parameter with the contribution of the higher-order distortions is eventually written as

$$\Phi(\mathbf{r}) = \sum_j \Psi_j(\mathbf{r}) = \sum_j \Psi_j \exp[iq_j\mathbf{G}_{002}\mathbf{r}]. \quad (1)$$

## III. GINZBURG-LANDAU FREE ENERGY IN THE SUCCESSIVE TRANSITIONS

As in cases of long period superlattices in alloys and an incommensurate-to-commensurate transition in barium sodium niobate,<sup>16-20</sup> we start with the following free-energy functional, using  $\bar{q} = \frac{1}{3}(1 - \bar{\delta})$ ,

$$F = \int d\mathbf{r} [K |(\nabla - i\bar{q}\mathbf{G}_{002})\Phi(\mathbf{r})|^2 + a\eta^2 + b\eta^3 + c\eta^4], \quad (2)$$

where the real order parameter having the higher-order distortions is given as  $\eta(\mathbf{r}) = \text{Re}[\Phi(\mathbf{r})]$  and  $\bar{\delta}$  is an incommensurability at  $T_f$ . In the present theory, we take into account only the translational symmetry for an invariance of the above free-energy functional. Coefficients

should be then given by, for instance,  $a = a_0 + \sum_{G_m} a_m \exp(-i\mathbf{G}_m \mathbf{r})$ . The temperature dependence of the coefficient is assumed only for  $a_0 = a'_0(T - T_0)$ . A general free energy is obtained by substituting Eq. (1) into Eq. (2) and can be written as

$$F = \sum_j \sum_{j'} K \psi_j \psi_{j'} (q_j - \bar{q})(q_{j'} - \bar{q}) G_{002}^2 \zeta(q_j - q_{j'}) + \frac{1}{4} \sum_j \sum_{j'} a \psi_j \psi_{j'} \zeta(q_j + q_{j'}) + \frac{1}{8} \sum_j \sum_{j'} \sum_{j''} b \psi_j \psi_{j'} \psi_{j''} \zeta(q_j + q_{j'} + q_{j''}) + \frac{1}{16} \sum_j \sum_{j'} \sum_{j''} \sum_{j'''} c \psi_j \psi_{j'} \psi_{j''} \psi_{j'''} \zeta(q_j + q_{j'} + q_{j''} + q_{j'''}) \quad (3)$$

where  $\zeta(q_j) = 1$  for  $q_j \mathbf{G}_{002} = 0$  or  $\mathbf{G}_m$  and  $\zeta(q_j) = 0$  otherwise. In Eq. (3), the coefficients are treated in the following rule, for instance,

$$a = \begin{cases} a_0 & \text{for } (q_j + q_{j'}) \mathbf{G}_{002} = 0, \\ a_m & \text{for } (q_j + q_{j'}) \mathbf{G}_{002} = \mathbf{G}_m. \end{cases} \quad (4)$$

It is worth noticing that Eq. (3) is the same free energy as Iizumi, Axe, and Shirane used in the analysis of the transitions in  $K_2SeO_4$ .<sup>1</sup> A feature of the present free energy is that the free energy has only terms up to the fourth-order ones.

From a series of our studies on the incommensurate phases,<sup>16-20</sup> we have recognized that features of the incommensurate phases such as the temperature dependence of the incommensurability can be well explained using only a several higher-order distortions, although the theory requires a lot of the distortions in order to get the lowest free energy. Three higher-order lattice distortions, the second-, fourth- and fifth-order distortions, were mainly used in the present analysis because a four-wave calculation was understood to reproduce a change in  $\delta$  with respect to temperature well. Note that experimentally only the second-order peak was observed in  $K_2SeO_4$ .<sup>1</sup> When the complex amplitude is written as  $\psi_j = \phi_j \exp(i\alpha_j)$  using both a real amplitude  $\phi_j$  and a phase  $\alpha_j$ , the free energy of the incommensurate phases for the four-wave case becomes

$$F_I = \kappa_0 \phi_0^2 + \kappa_{-1} \phi_{-1}^2 + \kappa_1 \phi_1^2 + \kappa_{-2} \phi_{-2}^2 - B_1 (\phi_0^2 \phi_{-1} + 2\phi_0 \phi_1 \phi_{-2} + \phi_{-1}^2 \phi_1) + C_1 (\phi_0^4 + \phi_{-1}^4 + \phi_1^4 + \phi_{-2}^4) + 4C_1 (\phi_0^2 \phi_{-1}^2 + \phi_0^2 \phi_1^2 + \phi_0^2 \phi_{-2}^2) + \phi_{-1}^2 \phi_1^2 + \phi_{-1}^2 \phi_{-2}^2 + \phi_1^2 \phi_{-2}^2 + \phi_0^2 \phi_{-1} \phi_1 + \phi_0 \phi_{-1}^2 \phi_{-2} + 2\phi_0 \phi_{-1} \phi_1 \phi_{-2} \quad (5)$$

with  $\kappa_j = K_0 (\delta_j - \bar{\delta})^2 G_{002}^2 + \frac{1}{2} a'_0 (T - T_0)$ . In the free energy, the phases are assumed to be  $\alpha_0 = \alpha_{-2} = 0$  and  $\alpha_{-1} = \alpha_1 = \pi$  without a loss of generality. Note that new coefficients  $\kappa_j$ ,  $B_1$ , and  $C_1$  are used in Eq. (5). The most important feature of the present free energy is that there are third-order umklapp terms  $-B_1 (\phi_0^2 \phi_{-1} + 2\phi_0 \phi_1 \phi_{-2} + \phi_{-1}^2 \phi_1)$ , which result from the condition of  $(q_j + q_{j'} + q_{j''}) \mathbf{G}_{002} = \mathbf{G}_{002}$ . As mentioned earlier, no fourth-order umklapp term exists in the free energy because the third-order distortion; that is, the polarization wave, is not taken into account in the present theory.

In our viewpoint, the commensurate phase has a wave vector of  $\mathbf{q}_c = \frac{1}{3} \mathbf{G}_{002}$  and there exists the third-order lock-in term in the free energy of the commensurate phase because of  $(q_j + q_{j'} + q_{j''}) \mathbf{G}_{002} = 3 \times \frac{1}{3} \mathbf{G}_{002} = \mathbf{G}_{002}$ . From Eq. (3), it is easy to write down the free energy of the commensurate phase as follows:

$$F_c = [K_0 \bar{\delta}^2 G_{002}^2 + \frac{1}{2} a'_0 (T - T_0)] \phi_c^2 - \frac{1}{3} B_1 \phi_c^3 + C_1 \phi_c^4, \quad (6)$$

where  $\phi_c$  is a real amplitude of the commensurate lattice distortion and a phase is assumed to be  $\alpha_c = \pi$ . Because

the commensurate phase exhibits the ferroelectric property, the free energy should have both the spontaneous polarization terms and the coupling term between the order parameter and the polarization. In spite of this fact, we do not consider these terms from the purpose of examining only the effect of the higher-order lattice distortions in the vicinity of the  $\frac{1}{3}$ -type position in the incommensurate phase.

The incommensurability  $\delta$  and the amplitude of the lattice distortion  $\phi_j$  at each temperature were determined by minimizing the free energy; for instance, Eq. (5) for the incommensurate phase and Eq. (6) for the commensurate phase in the four-wave case. An actual calculation was made in an iteration method. The phase modulation of the first-order lattice distortion is then calculated from determined amplitudes. In order to get a variation of the phase with respect to a position, the complex order parameter is converted into the following form:

$$\Phi(\mathbf{r}) = A(\mathbf{r}) \exp[i\{\frac{1}{3} \mathbf{G}_{002} \mathbf{r} + \Theta(\mathbf{r})\}] \quad (7)$$

with

$$A(\mathbf{r}) = \sqrt{a(\mathbf{r})^2 + b(\mathbf{r})^2},$$

$$\Theta(\mathbf{r}) = \tan^{-1}[b(\mathbf{r})/a(\mathbf{r})], \quad (8)$$

where  $a(\mathbf{r}) = \sum_j \psi_j \cos(q_j \mathbf{G}_{002} \mathbf{r})$  and  $b(\mathbf{r}) = \sum_j \psi_j \sin(q_j \mathbf{G}_{002} \mathbf{r})$ . It is obvious that  $\Theta(\mathbf{r})$  represents the phase modulation of the first-order distortion. That is, we can understand the details of the phase modulation from the variation of  $\Theta(\mathbf{r})$  with respect to temperature.

#### IV. CALCULATED RESULTS

In the present work, the coefficients in the free energy,  $K_0$ ,  $B_1$ , and  $C_1$ , were determined from a comparison between calculated and measured incommensurabilities. Note that the coefficient  $a'_0$  is assumed to be a unity. We then represent a calculated change in  $\delta$  first. Figures 2, 3, and 4 show calculated changes in  $\delta$  for  $\text{K}_2\text{SeO}_4$ ,  $\text{K}_2\text{ZnCl}_4$ , and  $\text{Rb}_2\text{ZnCl}_4$ , respectively, together with measured values of  $\delta$  at various temperatures.<sup>1,8</sup> Both values of  $T$  and  $\delta$  are normalized with respect to those at the normal-to-incommensurate transition, respectively. The measured values just below  $T_I$  are also omitted because of an inaccuracy resulting from a weak intensity. As can be seen in these figures, the theory reproduces the measured values very well in higher-temperature regions of the incommensurate phases, but cannot explain them in lower-temperature ones. It is obvious that this discrepancy comes from the incommensurate-to-commensurate transition. Among these materials, free energy curves of the incommensurate and commensurate phases for  $\text{K}_2\text{SeO}_4$  are, as an example, shown in Fig. 5. The calculation of the free energy curves was made using the same coefficients as those for the incommensurability. As is seen in Fig. 5, the curve of the commensurate phase inter-

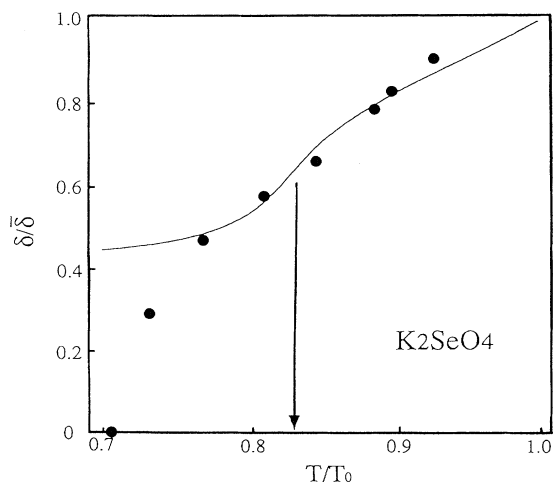


FIG. 2. Calculated incommensurability  $\delta$  as a function of the reduced temperature  $T/T_0$  for  $\text{K}_2\text{SeO}_4$ , together with measured values denoted by closed circles at various temperatures (Ref. 1). The value of  $\delta$  is normalized with respect to that at the transition temperature of the normal-to-incommensurate transition  $\bar{\delta}$ . The lock-in transition predicted on the basis of the present theory is also indicated by a long arrow.

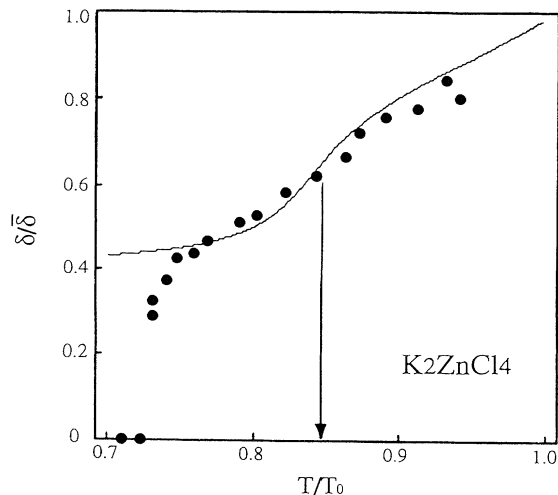


FIG. 3. Calculated incommensurability  $\delta/\bar{\delta}$  as a function of the reduced temperature for  $\text{K}_2\text{ZnCl}_4$ . In the figure, the measured value of  $\delta$  at each temperature is also plotted by a closed circle (Ref. 8). The predicted lock-in transition is indicated by a long arrow.

sects that of the incommensurate one at  $T/T_0 = 0.83$ , 108 K. This means that the theory predicts the first-order lock-in transition at 108 K. In Figs. 2–4, the predicted lock-in transitions are indicated by long arrows. An important feature of the lock-in transition is that the predicted transition temperature  $T_c^i$  is higher than the measured one  $T_c^m$ . In spite of this disagreement, however the present theory is basically understood to explain the change in the incommensurability for  $\text{K}_2\text{SeO}_4$ ,  $\text{K}_2\text{ZnCl}_4$ , and  $\text{Rb}_2\text{ZnCl}_4$ . Determined coefficients and  $T_c^i$  for each material are listed in Table I, together with an experimentally obtained transition temperature of the normal-

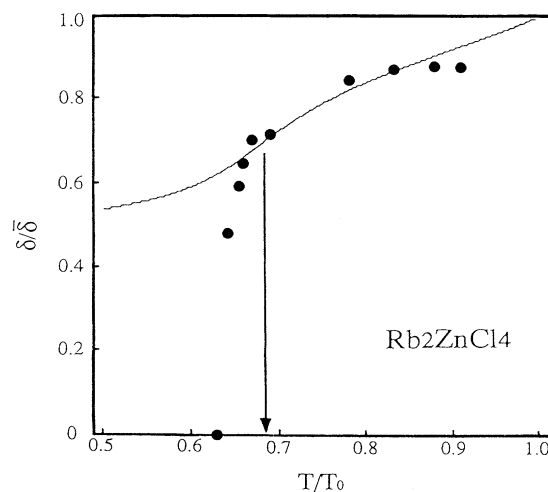


FIG. 4. Calculated incommensurability  $\delta/\bar{\delta}$  as a function of the reduced temperature for  $\text{Rb}_2\text{ZnCl}_4$ , together with measured values denoted by closed circles (Ref. 8). The predicted lock-in transition is indicated by a long arrow.

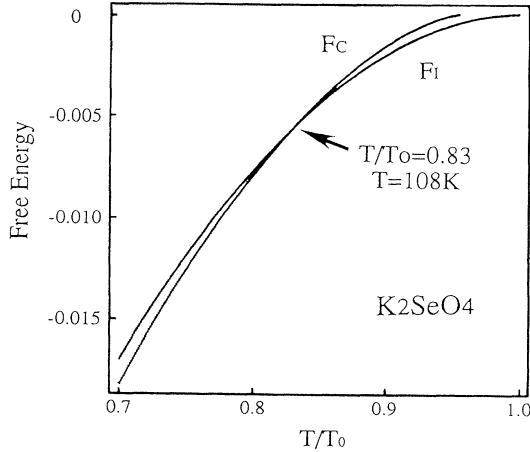


FIG. 5. Temperature dependence of the free-energy curves for the incommensurate phase ( $F_I$ ) and the commensurate one ( $F_C$ ) in  $K_2SeO_4$ . The temperature is normalized with respect to  $T_0$ .

to-incommensurate transition,  $T_I^m$ , and that of the incommensurate-to-commensurate one,  $T_c^m$ . The disagreement between  $T_c^t$  and  $T_c^m$  will be discussed later.

Because determined magnitudes for each coefficient are almost the same in  $K_2SeO_4$ ,  $K_2ZnCl_4$ , and  $Rb_2ZnCl_4$ , calculated changes in amplitudes of the first-, second-, fourth-, and fifth-order lattice distortions should also resemble one another. From this fact, we present them only in  $K_2SeO_4$  here. Calculated changes in the amplitudes of the first- and higher-order distortions in  $K_2SeO_4$  are depicted in Fig. 6. In the figure, a square root of a measured peak intensity at each temperature, which was obtained by Iizumi, Axe, and Shirane,<sup>1</sup> is also plotted by a closed circle. The root is normalized with respect to that at  $T/T_0=0.80$ , 104 K. It is understood that the calculated amplitude of the first-order distortion increases with decreasing temperature and is in very good agreement with the measured value. As for the higher-order distortions, when the temperature is lowered from  $T_I$ , the amplitudes of the distortions increase gradually and exhibit a relatively large change around  $T_c^t$ . At  $T/T_0=0.90$ , for instance, the amplitudes of the second-, fourth-, and fifth-order distortions with respect to  $\phi_0$  are, respectively, determined to be  $\phi_{-1}/\phi_0=0.178$ ,  $\phi_1/\phi_0=-0.048$ , and  $\phi_{-2}/\phi_0=-0.004$ . Because a rela-

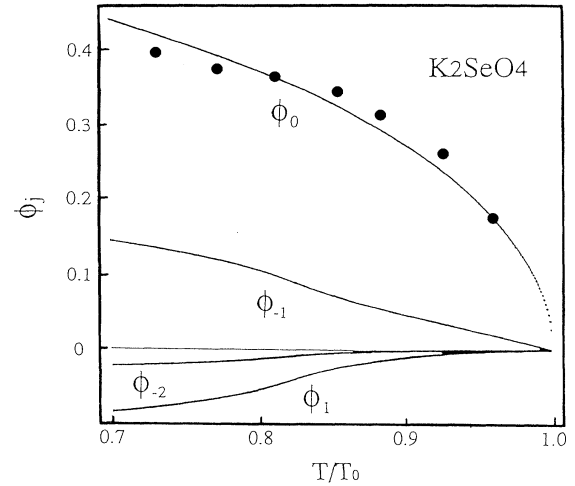


FIG. 6. Determined magnitudes of the real amplitudes of the first- and higher-order distortions as a function of  $T/T_0$  for  $K_2SeO_4$ . The amplitudes of the first-, second-, fourth-, and fifth-order distortions are represented by  $\phi_0$ ,  $\phi_{-1}$ ,  $\phi_1$ , and  $\phi_{-2}$ , respectively. A solid circle at each temperature also denotes an amplitude obtained as a square root of the measured intensity of the first-order peak (Ref. 1).

tive intensity is proportional to  $(\phi_j/\phi_0)^2$ , the fourth-, and fifth-order peaks among the higher-order ones have very weak intensities against the first-order one. It is then hard to detect diffraction peaks due to these distortions experimentally. On the other hand, the second-order peak should be detected because of  $(\phi_{-1}/\phi_0)^2 \sim 0.032$ . Neutron diffraction actually showed the second-order peak although the measured peak intensity is weaker than the intensity predicted by the present theory.<sup>1</sup>

In order to understand the details of the phase and amplitude modulations, we calculated these modulations using the determined amplitudes. The present calculation showed that the change in the phase modulation in  $K_2ZnCl_4$  is identical to that in  $K_2SeO_4$ . We then show the variation of the phase against the position for both  $K_2SeO_4$  and  $Rb_2ZnCl_4$ . Figure 7 represents relations between the phase  $\Theta$  and the position  $r$  at four temperatures,  $T/T_0=0.97$ , 0.90, 0.83, and 0.77, in  $K_2SeO_4$ . The position in the figure is normalized with respect to a distance between two neighboring discommensurations at  $T/T_0=0.77$ ,  $\Delta r$ . At  $T/T_0=0.97$ , the relation is almost a straight line and the phase modulation does not basically occur. When the temperature is lowered, the relation becomes a steplike shape. Actually, the relation at  $T/T_0=0.77$  below  $T_c^t$  consists of both in-phase and phase-slip regions, which are indicated by  $A$  and  $B$ , respectively. It is obvious that the phase-slip region should be identified as the discommensuration. A feature of the discommensuration is that the phase slip does not take place at a point in space, but occurs gradually in a finite distance. Because of the gradual change in the phase, we call the phase-slip region the extended discommensuration. A magnitude of the phase slip is found to be  $2\pi/3$ . In addition, the relation at  $T/T_0=0.83$  does not exhibit

TABLE I. Determined values of three coefficients,  $K_0 G_{002}^2$ ,  $B_1$ , and  $C_1$ , in the free energy and the predicted transition temperature of the lock-in transition  $T_c^t$  for  $K_2SeO_4$ ,  $K_2ZnCl_4$ , and  $Rb_2ZnCl_4$ . The transition temperatures of the normal-to-incommensurate and lock-in transitions,  $T_I^m$  and  $T_c^m$ , which were determined experimentally, are also listed.

Material	$K_0 G_{002}^2$	$B_1$	$C_1$	$T_c^t$ (K)	$T_I^m$ (K)	$T_c^m$ (K)
$K_2SeO_4$	0.034	0.40	0.44	108	130	91
$K_2ZnCl_4$	0.032	0.39	0.44	470	553	404
$Rb_2ZnCl_4$	0.034	0.27	0.38	209	303	191

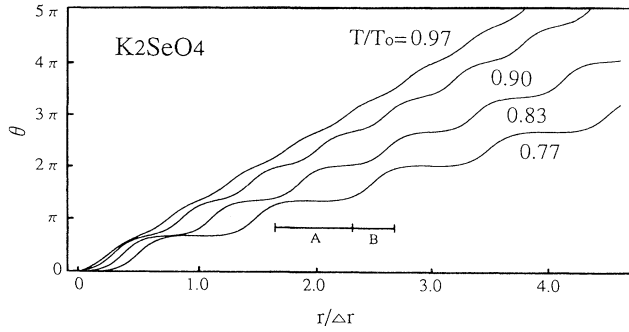


FIG. 7. Position dependence of the phase  $\Theta$  of the modulated first-order distortion at  $T/T_0=0.97, 0.90, 0.83,$  and  $0.77$  for  $K_2SeO_4$ . The position is normalized with respect to a distance between two neighboring discommensurations at  $T/T_0=0.77, \Delta r$ . In the figure, the in-phase and the discommensuration are indicated by  $A$  and  $B$ , respectively.

the in-phase region defined as  $d\Theta/dr=0$ . This means that the discommensuration is not well developed at  $T_c^t$ . It should be remarked that in Fig. 2 the measured incommensurability deviates from the calculated one below  $T/T_0=0.77$ , at which the discommensuration is sufficiently developed, as mentioned just above. Figure 8 shows relations between the phase and the position at  $T/T_0=0.80, 0.68,$  and  $0.63$  in  $Rb_2ZnCl_4$ . Although the change in the relation with respect to temperature is basically the same as that for  $K_2SeO_4$ , the in-phase region with  $d\Theta/dr=0$  does not form even at  $T_c^m$  of  $T/T_0=0.63$  below  $T_c^t$  of  $T/T_0=0.68$  in  $Rb_2ZnCl_4$ .

There is no essential difference in a calculated amplitude modulation for  $K_2SeO_4, K_2ZnCl_4,$  and  $Rb_2ZnCl_4$ . Figure 9 represents relations between the amplitude and the position at three temperatures,  $T/T_0=0.90, 0.83,$  and  $0.77$ , only in  $K_2SeO_4$ . Note that in Fig. 9 we used the normalized position, just as in the case of the phase modulation. In Fig. 9, there are minima in the amplitude at the discommensurations, which correspond to the out-of-phase region. When the temperature is lowered, a size of a region with a constant amplitude is enlarged and other minima in the amplitude then appear at the middle of the in-phase region below  $T_c^t$ . In other words, the

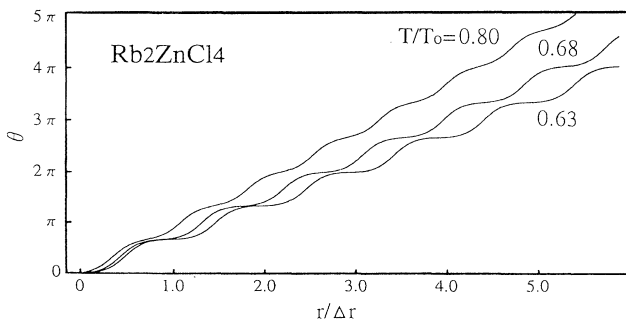


FIG. 8. Position dependence of the phase  $\Theta$  at  $T/T_0=0.80, 0.68,$  and  $0.63$  for  $Rb_2ZnCl_4$ . The position is normalized with respect to a distance between two neighboring discommensurations at  $T_c^m$  of  $T/T_0=0.63, \Delta r$ .

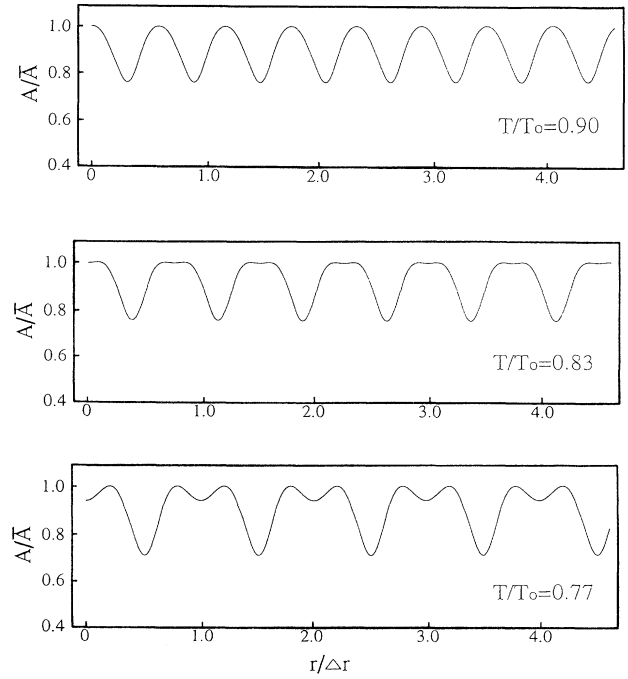


FIG. 9. Position dependence of the amplitude  $A$  at  $T/T_0=0.90, 0.83, 0.77$  for  $K_2SeO_4$ . The amplitude and the position are, respectively, normalized with respect to the maximum value of the amplitude  $\bar{A}$  and a distance between two neighboring discommensurations at  $T/T_0=0.77, \Delta r$ .

constant-amplitude region has a maximum size around  $T_c^t$ .

Eventually we show a modulated first-order distortion,  $\eta(r)$  with the contribution of the higher-order distortions, at  $T/T_0=0.77$  for  $K_2SeO_4$  in Fig. 10. As is understood in the figure, in order to get the lower free energy of the incommensurate phase, the in-phase region with the commensurate period is enlarged in space and the out-of-phase region identified as the discommensuration is shrunk. The amplitude of the distortion is also reduced at the discommensuration. Further, there exists a slight decrease in the amplitude in the middle of the in-phase region although the discommensuration is well developed.

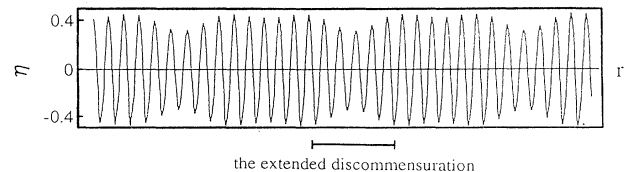


FIG. 10. Variation of the real order parameter with the contribution of the higher-order distortions against the position at  $T/T_0=0.77$  for  $K_2SeO_4$ .

## V. DISCUSSION

The present Ginzburg-Landau theory considering only the higher-order lattice distortions near the first-order one are in reciprocal space clearly shows that the incommensurate features such as the change in the incommensurability in  $K_2SeO_4$ ,  $K_2ZnCl_4$ , and  $Rb_2ZnCl_4$ , which have been obtained experimentally, originate mainly from the phase modulation of the first-order distortion by means of the higher-order ones. The phase modulation is an effort of a crystal to obtain the lower free energy of the incommensurate phase. Note that the lattice distortions are due to the rotation of the tetrahedron involved in the crystal structure as the modulation mode. As a result of the phase modulation, the discommensuration with the phase slip of  $2\pi/3$  is developed in lower temperatures of the incommensurate phases. Because of the phase slip of  $2\pi/3$ , the patterns consisting of three discommensurations should play an important role in the incommensurate-to-commensurate transition. On the other hand, a problem of the present theory is that the calculated transition temperature of the incommensurate-to-commensurate transition,  $T_c^t$ , is higher than the measured temperature,  $T_c^m$ . The details of the incommensurate-to-commensurate transition will be mainly discussed here.

The incommensurate-to-commensurate transitions in  $K_2SeO_4$ ,  $K_2ZnCl_4$ , and  $Rb_2ZnCl_4$  are understood to be of the first order according to the present theory. In addition, the spontaneous polarization has been observed only in the commensurate phase. The lock-in transition then involves the following four processes; that is, the nucleation and growth of the ferroelectric commensurate phase and the formation and annihilation of the pattern consisting of the discommensurations. The latter processes are directly related to the rapid decrease in the incommensurability in the transition. It should be remarked that these processes are characterized as a thermally activated process and were actually observed in  $Rb_2ZnCl_4$  by transmission electron microscopy.<sup>7</sup> It is obvious that the existence of the thermally activated processes leads to the fact that  $T_c^m$  obtained in the cooling process should be lower than  $T_c^t$ . Although we do not know whether  $T_c^m$  in  $K_2SeO_4$  and  $K_2ZnCl_4$  was experimentally determined on cooling or heating, at least  $T_c^t$  is slightly higher than  $T_c^m$  obtained on heating in  $Rb_2ZnCl_4$ .<sup>21</sup> This fact clearly indicates that both the macroscopic polarization terms and the coupling term between the polarization and the order parameter must be taken into account in the free energy of the commensurate phase. It should be remarked that the consideration of these terms results in new coefficients as an adjustable parameter. The introduction of the new parameters must make the reproduction of  $T_c^m$  possible. In order to elucidate an essential origin of the incommensurate features, however the smallest number of the parameters should be adopted. Because of this, we take into account only the lattice distortions as an order parameter. Since even the present theory with only three parameters  $K_0$ ,  $B_1$ , and  $C_1$  can give a rough estimation of the transition temperature of the incommensurate-to-commensurate transition,

the incommensurate features are basically understood to be explained as being due to the phase modulation of the first-order distortion by the higher-order ones.

Because the discommensuration as the out-of-phase region leads to a loss of an elastic energy, the ferroelectric commensurate phase should be nucleated along the discommensuration. When one of two types of ferroelectric domains in a domain structure is nucleated along the discommensuration, the domain structure indicated by a thick solid lines in Fig. 11 must be formed in the incommensurate phase. Note that the dashed line denotes the calculated relation between the phase and the position at  $T/T_0=0.77$  for  $K_2SeO_4$ , which is shown in Fig. 7. As can be understood in Fig. 11, a size of a domain is almost the same as that of the discommensuration and one of two domains forming the domain structure plays a role of the discommensuration with the phase slip of  $2\pi/3$  against the other. In other words, a ferroelectric domain wall can be regarded as a discommensuration with a phase slip of  $2\pi/6$ . Therefore, the incommensurate-to-commensurate transition proceeds by the formation and annihilation of a pattern consisting of six ferroelectric domain walls, as was observed experimentally.<sup>5,7</sup> In this situation, further an external electric field helps both the nucleation of the ferroelectric commensurate phase and the annihilation of the pattern. The electric field should then result in an increase in the transition temperature of the incommensurate-to-commensurate transition.

As mentioned earlier, the calculated intensity of the second-order peak in  $K_2SeO_4$  is slightly stronger than the intensity measured by Iizumi, Axe, and Shirane,<sup>1</sup> although the intensity itself is very weak. We believe that this disagreement is not a serious problem in the present theory. In the comparison between the calculated and measured intensities, we used the peak intensities along the symmetry line. It should be noticed that the locations of the higher-order peaks in reciprocal space are very sensitive to a deviation of that of the first-order peak from the symmetry line. From this fact, we think that the disagreement is due to a slight deviation from the line and then a careful measurement of the intensity in a wide

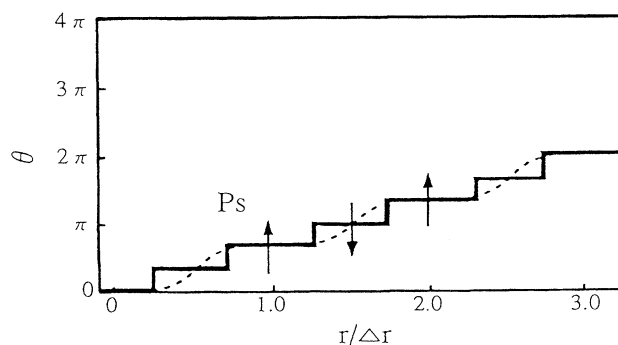


FIG. 11. Schematic representation of the ferroelectric domain structure appearing in the lock-in transition. In the figure, the expected domain structure is depicted by a thick solid line, while the dashed line shows the relation between the phase and the position at  $T/T_0=0.77$  for  $K_2SeO_4$ . A vector  $\mathbf{P}_s$  denotes a direction of the spontaneous polarization in the domain structure.

region of the reciprocal space is needed in order to measure integrated intensities of the higher-order peaks.

In the present work, the calculation was made for different numbers of the higher-order distortions  $N$  in the vicinity of the first-order one; concretely  $N = 1, 3$ , and  $7$ . The best fit with the observed features was obtained for  $N = 3$ , as was shown. This situation is entirely identical to all incommensurate phases, which we have analyzed so far.<sup>16-20</sup> We do not understand why the four-wave calculation ( $N = 3$ ) is the most appropriate to produce the features observed in the incommensurate phases. Because the lattice distortions are due to the rotation of the tetrahedron as the modulation mode, it seems that this fact is related to a discontinuity of a lattice system. The following should be noted. If a large number of the higher-order distortions were taken into account to obtain the lowest free energy, the incommensurate-to-commensurate transition would be of the second order. In other words, the experimental data require a limited number of higher-order lattice distortions.

Recently Chen and Walker analyzed successive transitions in the  $A_2BX_4$  family in terms of competing interactions and obtained a behavior characterized as the devil's staircase for the appearance of various incommensurate and commensurate phases.<sup>10,22</sup> Their theory can explain

a lot of features in the successive transitions in the  $A_2BX_4$  family except for the incommensurate features such as phase modulation. On the other hand, our work is particularly focused on the incommensurate features. We believe that both types of the approaches are definitely needed to get a complete understanding of the successive transitions in the  $A_2BX_4$  family.

## VI. CONCLUSION

Among the  $A_2BX_4$  family, there exist the incommensurate phases with the commensurate phase characterized by the wave vector of  $\mathbf{q}_c = \frac{1}{3}\mathbf{G}_{002}$  in  $\text{K}_2\text{SeO}_4$ ,  $\text{K}_2\text{ZnCl}_4$ , and  $\text{Rb}_2\text{ZnCl}_4$ . We have analyzed the features observed in these incommensurate phases on the basis of the Ginzburg-Landau theory considering the contribution of the higher-order lattice distortions. As a result, the features of the incommensurate phases were understood to result from the phase modulation of the first-order distortion by means of the higher-order ones. Eventually, the incommensurate phases in these materials are characterized as a pure discommensurate structure due to the rotation of the tetrahedron as the modulation mode without the ferroelectric domain structure.

<sup>1</sup>M. Iizumi, J. D. Axe, and G. Shirane, Phys. Rev. B **15**, 4392 (1977).

<sup>2</sup>K. Aiki, K. Hukuda, H. Koga, and T. Kobayashi, J. Phys. Soc. Jpn. **28**, 389 (1970).

<sup>3</sup>K. Shimaoka, N. Tsuda, and Y. Yoshimura, Acta Crystallogr. B **26**, 1451 (1972).

<sup>4</sup>K. Gesi and M. Iizumi, J. Phys. Soc. Jpn. **53**, 4271 (1984).

<sup>5</sup>H. Sakata, K. Hamano, X. Pan, and H.-G. Unruh, J. Phys. Soc. Jpn. **59**, 1079 (1990).

<sup>6</sup>S. R. Andrews and H. Mashiyama, J. Phys. C **16**, 4985 (1983).

<sup>7</sup>K. Tsuda, N. Yamamoto, and K. Yagi, J. Phys. Soc. Jpn. **57**, 2057 (1988).

<sup>8</sup>K. Gesi and M. Iizumi, J. Phys. Soc. Jpn. **46**, 697 (1979).

<sup>9</sup>H. Z. Cummins, Phys. Rep. **185**, 211 (1990).

<sup>10</sup>Z. Y. Chen and M. B. Walker, Phys. Rev. B **43**, 5634 (1991).

<sup>11</sup>W. L. McMillan, Phys. Rev. B **14**, 1496 (1976).

<sup>12</sup>K. Aizu, J. Phys. Soc. Jpn. **43**, 188 (1977).

<sup>13</sup>K. Gesi, J. Phys. Soc. Jpn. **61**, 1225 (1992).

<sup>14</sup>S. Sawada, Y. Shiroishi, A. Yamamoto, M. Takashige, and M. Matsuo, J. Phys. Soc. Jpn. **43**, 2099 (1977).

<sup>15</sup>K. Hamano, Y. Ikeda, T. Fujimoto, K. Ema, and S. Hirotsu, J. Phys. Soc. Jpn. **49**, 2278 (1980).

<sup>16</sup>Y. Koyama, Z. P. Zhang, and H. Sato, Phys. Rev. B **36**, 3701 (1987).

<sup>17</sup>Y. Koyama, J. Yoshida, H. Hoshiya, and Y. Nakamura, Phys. Rev. B **40**, 5378 (1989).

<sup>18</sup>Y. Koyama and M. Ishimaru, Phys. Rev. B **41**, 8522 (1990).

<sup>19</sup>Y. Koyama and S. Mori, Phys. Rev. B **44**, 7852 (1991).

<sup>20</sup>S. Mori, Y. Koyama, and Y. Uesu, Phys. Rev. B **49**, 621 (1994).

<sup>21</sup>H. Mashiyama, S. Tanisaki, and K. Hamano, J. Phys. Soc. Jpn. **51**, 2538 (1982).

<sup>22</sup>Z. Y. Chen and M. B. Walker, Phys. Rev. Lett. **65**, 1223 (1990).